



Ancient genomes reveal tropical bovid species in the Tibetan Plateau contributed to the prevalence of hunting game until the late Neolithic

Ningbo Chen^{a,b,1}, Lele Ren^{c,1}, Linyao Du^{d,1}, Jiawen Hou^{b,1}, Victoria E. Mullin^e, Duo Wu^d, Xueye Zhao^f, Chunmei Li^{a,g}, Jiahui Huang^{a,h}, Xuebin Qi^{a,g}, Marco Rosario Capodiferroⁱ, Alessandro Achilliⁱ, Chuzhao Lei^b, Fahu Chen^j, Bing Su^{a,g,2}, Guanghui Dong^{d,j,2}, and Xiaoming Zhang^{a,g,2}

^aState Key Laboratory of Genetic Resources and Evolution, Kunming Institute of Zoology, Chinese Academy of Sciences (CAS), 650223 Kunming, China; ^bKey Laboratory of Animal Genetics, Breeding and Reproduction of Shaanxi Province, College of Animal Science and Technology, Northwest A&F University, 712100 Yangling, China; ^cSchool of History and Culture, Lanzhou University, 730000 Lanzhou, China; ^dCollege of Earth and Environmental Sciences, Lanzhou University, 730000 Lanzhou, China; ^eDepartment of Earth Sciences, Natural History Museum, London SW7 5BD, United Kingdom; ^fGansu Provincial Institute of Cultural Relics and Archaeology, 730000 Lanzhou, China; ^gCenter for Excellence in Animal Evolution and Genetics, Chinese Academy of Sciences, 650223 Kunming, China; ^hKunming College of Life Science, University of Chinese Academy of Sciences, 100049 Beijing, China; ⁱDipartimento di Biologia e Biotechnologie "L. Spallanzani," Università di Pavia, 27100 Pavia, Italy; and ^jCAS Center for Excellence in Tibetan Plateau Earth Sciences, Institute of Tibetan Plateau Research, Chinese Academy of Sciences, 100101 Beijing, China

Edited by Zhonghe Zhou, Chinese Academy of Sciences, Beijing, China, and approved September 11, 2020 (received for review June 7, 2020)

Local wild bovids have been determined to be important prey on the northeastern Tibetan Plateau (NETP), where hunting game was a major subsistence strategy until the late Neolithic, when farming lifestyles dominated in the neighboring Loess Plateau. However, the species affiliation and population ecology of these prehistoric wild bovids in the prehistoric NETP remain unknown. Ancient DNA (aDNA) analysis is highly informative in decoding this puzzle. Here, we applied aDNA analysis to fragmented bovid and rhinoceros specimens dating ~5,200 y B.P. from the Neolithic site of Shannashuzha located in the marginal area of the NETP. Utilizing both whole genomes and mitochondrial DNA, our results demonstrate that the range of the present-day tropical gaur (*Bos gaurus*) extended as far north as the margins of the NETP during the late Neolithic from ~29°N to ~34°N. Furthermore, comparative analysis with zooarchaeological and paleoclimatic evidence indicated that a high summer temperature in the late Neolithic might have facilitated the northward expansion of tropical animals (at least gaur and Sumatran-like rhinoceros) to the NETP. This enriched the diversity of wildlife, thus providing abundant hunting resources for humans and facilitating the exploration of the Tibetan Plateau as one of the last habitats for hunting game in East Asia.

ancient DNA | northeastern Tibetan Plateau | *Bos gaurus* | late Neolithic | hunting game

Interactions among climate change, biogeography, and human activity have remarkably strengthened since the late Pleistocene. Abrupt climate change is attributed as a significant factor in worldwide human dispersal (1, 2) and the transformation of megafauna in the Arctic region in the late Pleistocene (3) and contributed to the agricultural revolution in the early Holocene (4). Farmers diffused across the Old World with crops and livestock during the Neolithic period (~10,000 to 4,000 y B.P.) (5), eventually affecting the biogeography in Eurasia (6). However, the impact of the geographical distribution of wildlife on human behavior during that period remains enigmatic.

In East Asia, millet crops were domesticated ~10,000 y B.P. (7), with a millet-based agricultural lifestyle established in the Loess Plateau ~6,000 y B.P. (8). The millet farmers of the late Yangshao (5,500 to 5,000 y B.P.) and Majiayao (5,300 to 4,000 y B.P.) cultures expanded westward to the northeastern Tibetan Plateau (NETP) and settled extensively below 2,500 m above sea level (m a.s.l.) (9–11). Even after the introduction of agriculture to the NETP over 1,200 y B.P., hunting game remained a major subsistence strategy for the indigenous Zongri societies (~5,300 to 4,000 y B.P.) (12) that inhabited the plateau between 2,800

and 3,000 m a.s.l. Therefore, the NETP served as one of the last habitats for the prevalence of hunting strategies in East Asia.

In contrast with previous zooarchaeological studies on early Majiayao groups, abundant wild faunal remains were unearthed from the early Majiayao site of Shannashuzha (SNSZ) (34°29' 34.06"N, 104°4'24.54"E Min County, Gansu Province), which is dated to ~5,280 to 5,050 y B.P. and located in the marginal area of the NETP at 2,323 m a.s.l. (13). The proportion of the identified wildlife remains (~76%) far exceeded domestic animals (pig and dog) (~24%) (14), while the plant remains were dominated by carbonized foxtail and broomcorn grains (over 80%) (13, 15). This suggests that both millet cultivation and game hunting occurred at SNSZ, despite previous zooarchaeological studies suggesting that early Majiayao groups mainly utilized livestock rather than wildlife for meat protein consumption (16).

Significance

We undertook an ancient genomic DNA investigation of large animal remains dated ~5,200 y B.P. from the Tibetan Plateau. We provide compelling evidence that the present-day low-latitude tropical inhabitants *Bos gaurus* and *Dicerorhinus sumatrensis* once roamed as far north as the margin of the northeastern Tibetan Plateau (NETP) during the late Neolithic, pushing the historical gaur distribution from ~29°N to ~34°N. Further multidisciplinary exploration indicates that a high summer temperature in the late Neolithic might have facilitated the northward expansion of these tropical animals to the NETP, which enriched the biodiversity of wildlife and contributed to the exploration of the Tibetan Plateau as one of the last habitats for hunting game in East Asia.

Author contributions: B.S., G.D., and X. Zhang designed research; J. Hou, C. Li, J. Huang, X.Q., C. Lei, F.C., B.S., G.D., and X. Zhang performed research; N.C., L.D., V.E.M., D.W., X. Zhao, C. Li, and M.R.C. contributed new reagents/analytic tools; N.C., L.R., L.D., J. Hou, V.E.M., D.W., X. Zhao, M.R.C., A.A., and X. Zhang analyzed data; and N.C., L.R., L.D., V.E.M., C. Lei, F.C., G.D., and X. Zhang wrote the paper.

The authors declare no competing interest.

This article is a PNAS Direct Submission.

This open access article is distributed under [Creative Commons Attribution-NonCommercial-NoDerivatives License 4.0 \(CC BY-NC-ND\)](https://creativecommons.org/licenses/by-nc-nd/4.0/).

¹N.C., L.R., L.D., and J.H. contributed equally to this work.

²To whom correspondence may be addressed. Email: zhangxiaoming@mail.kiz.ac.cn, ghdong@lzu.edu.cn, or sub@mail.kiz.ac.cn.

This article contains supporting information online at <https://www.pnas.org/lookup/suppl/doi:10.1073/pnas.2011696117/-DCSupplemental>.

First published October 19, 2020.

The wild animal remains at SNSZ include bones of deer (*Cervidae*), gorals (*Nemorhaedus griseus*), snub-nosed monkeys (*Rhinopithecus roxellana*), and rhinoceroses (*Dicerorhinus*). Bovid remains have also been identified at SNSZ and they were tentatively recognized as Tibetan yak or domestic cattle. However, they are too degraded for species identification using morphological approaches (14). Ancient DNA (aDNA) is a powerful tool for identifying bovid remains from archaeological sites in northern China, including domestic cattle (*Bos taurus*), wild water buffalo (*Bubalus mephistopheles*), and aurochs (*Bos*

primigenius) (17–20). Although bovid remains have been frequently identified in many prehistoric sites on the Tibetan Plateau (7, 9, 12, 21), the species-level identification of bovid species on the Tibetan Plateau has not been reported.

Using aDNA profiles, we provide compelling evidence that ~5,200 y B.P. the range of the present-day tropical gaurs (*Bos gaurus*) and Sumatran-like rhinoceroses (*Dicerorhinus sumatrensis*) extended as far north as the margins of the NETP at the northernmost latitude of 34.49°N. During this period the mean annual and summer temperatures in the Northern Hemisphere,

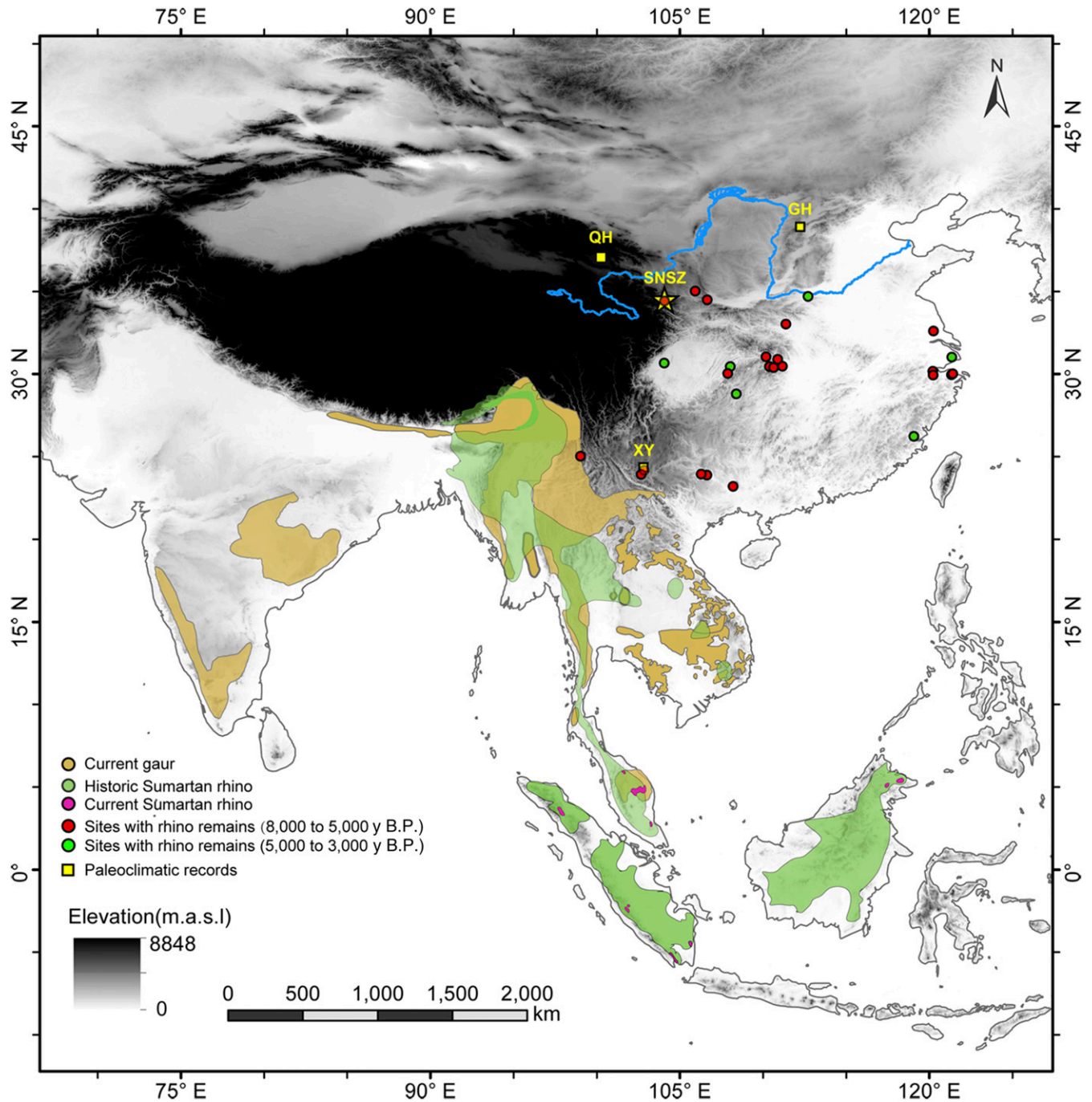


Fig. 1. The distribution of gaur and Sumatran rhinos in Asia and the location of the SNSZ site. Differently colored regions represent the historic and modern distribution of the two species. The historical distribution of Sumatran rhinos was derived from range maps in Foose et al. (27), and the current distribution was derived from IUCN (2008) (26). The current distribution of gaur was derived from IUCN (25). SNSZ represents the Shannashuzha site, GH represents Gonghai Lake, XY represents Xingyun Lake, and QH represents Qinghai Lake.

especially in the middle-high latitude regions, were much higher than those during the preindustrial period (e.g., the 19th century) (22–24). These two tropical species currently inhabit low-latitude tropical or subtropical regions; however, to our knowledge (25–27), no other evidence has shown that the modern gaur's range previously expanded into northern China. Therefore, our results provide evidence for revisiting the connection between climate change, biogeographic distributions, and the geographical patterns of human subsistence strategies in East Asia during the late Neolithic period.

Results

aDNA Authenticity, Preservation, and Radiocarbon Dating of Bovid Faunal Remains from the SNSZ Site. The SNSZ archeological site is located in Min County, Gansu Province, the margin of the NETP. The site is adjacent to the Tao River, which is a tributary of the upper Yellow River, with surrounding high mountainous terrain to the northeast and southwest (Fig. 1). Between 1981 and 2010, the meteorological station records of Min County, which lies at an elevation of 2,315 m a.s.l. and a distance ~26 km south of the site (www.nmic.cn), documented a mean annual temperature of ~6.5 °C, a mean summer temperature of 15.5 °C, and a mean annual precipitation of ~556 mm.

According to the excavated artifacts and cultural relics, the community of the SNSZ site is regarded as the early phase of Majiayao culture, which was a late Neolithic culture that prevailed 5,300 to 4,000 y B.P. in the NETP around the valley of the upper Yellow River (16). Systematic archaeological surveys of the SNSZ reported typical mountain vegetation including conifer forests, mixed broadleaved/conifer forests, riverbank broadleaved forests, and, in particular, an abundant Bambusoideae botanical composition (14, 28). In addition, zooarchaeological classification identified a significantly higher proportion (>76%) of the number of identified specimens (NISP) of wild animal remains than of domestic animals (13) (*SI Appendix, Figs. S1 and S2 and Table S1*), which include tropical inhabiting species such as bamboo rats (*Rhizomys pruinosus*), rhinoceroses (*Diceros rhinus*), and considerable unknown bovid remains (14) (*SI Appendix, Fig. S1*). However, the species affiliation of these bovid bones is unknown due to the morphological overlap among bovid species' faunal remains. We performed accelerator mass spectrometry (AMS) radiocarbon dating for five selected animal bones from the SNSZ site, including one bovid bone for species identification, and the ¹⁴C dating ranged from ~5,280 to 5,050 y B.P. (Table 1).

We performed the aDNA laboratorial work in the aDNA dedicated laboratory of the Comparative Genomic Group (CGG) at Kunming Institute of Zoology, Chinese Academy of Sciences. Using the initial shotgun-sequencing screen data, we first assessed the aDNA authenticity and preservation situation by evaluating several key indexes, including the terminal damage rate (TDR) (*SI Appendix, Fig. S3*), the average fragmental length, and the mapping rate (*SI Appendix, Table S2*). The TDRs for all 10 samples were ≥10%, and the average fragmental

lengths and the mapping rates range from 56 bp to 80 bp and 0.001 to 3.75%, respectively (*SI Appendix, Table S2*), all of which indicate that all samples have molecular characteristics typical of aDNA. In addition, for the captured sequence data, we plotted the sequence fragmental size distribution for each sample, indicating a short fragment enrichment pattern, which serves as the typical pattern of aDNA (*SI Appendix, Fig. S4*).

Molecular Identification of Species Affiliation Reveals the Present-Day Tropical Rainforest-Inhabiting Gaur and Sumatran Rhinoceros Once Roamed over the NETP ~5,200 y B.P.

We collected 10 bone samples to perform molecular identification of these bovid faunal remains from the SNSZ site (*SI Appendix, Fig. S1 and Table S2*). Identification of the bovid specimens was first achieved through mitochondrial DNA (mtDNA) analysis, with all 10 samples aligning the most reads to the modern-day gaur (NC_024818.1) mitogenome, as opposed to other bovid species such as the yak or domestic taurine cattle. By combining the shotgun and capture sequenced data, we obtained mtDNA genomes from 5.8× to 1,703.5× (median depth of 327.65×) (*SI Appendix, Table S3*). To further determine the species affiliation, we analyzed these bovid mtDNA sequences together with the currently known matrilineal variability of nine modern Bovini species (taurine cattle [*B. taurus*], zebu [*Bos indicus*], gaur [*B. gaurus*], gayal [*Bos frontalis*], banteng [*Bos javanicus*], yak [*Bos grunniens*], American bison [*Bison bison*], European bison [*Bison bonasus*], and water buffalo [*Bubalus bubalis*]) (*SI Appendix, Table S4*). Both the constructed maximum likelihood (ML) and the Bayesian phylogenetic trees confirmed the placement of the 10 SNSZ bovinds as sister lineages to the modern gaurs and gayals. (Fig. 2 A–C). The 20 gaur and gayal mtDNA sequences clustered into three divergent haplogroups, which we named G1, G2, and G3. Moreover, we found that 9 of the 10 ancient samples were tightly clustered together (G3) and diverged from the living gaur and gayal lineages (G2) ~18,000 y B.P. (Fig. 2C), which is suggestive of a possible extinct sublineage with deep divergence from the modern lineages. However, one individual, H63, was closer to the modern gaur and gayal lineages (G2a) compared to other individuals and showed an ancestry state to the modern lineages, which is an indication of a possible transitional population between the “northern” and “southern” gaurs (Fig. 2C). The relatively young ages of G2a and G3 and their star-like features could be connected to an expansion that might have occurred after the Last Glacial Maximum (LGM, 25,000 to 18,000 y B.P.).

To corroborate the above species identification and further explore the population relationships, we mapped the genome-capture data from the 10 samples to the taurine cattle reference genome (ARS-UCD1.2). We obtained genomic nuclear DNA data with sequence depths ranging from 0.12× to 3.73× (median 1.16×). We found that these 10 samples included five male and five female samples, respectively (*SI Appendix, Table S2*). For the three relatively higher-genomic-coverage samples, H113, H57, and H48, we found that they possessed fourth- to third-generation

Table 1. Calibrated radiocarbon dates of animal bones from the excavation of the SNSZ site

Laboratory no.	Provenience	Dating method	Dating material	Radiocarbon age, y B.P.	Calibrated age, cal y B.P.	
					1σ (68.2%)	2σ (95.4%)
LZU149	2013MCSIT0309⑤	AMS	Collagen from Cervidae	4,510 ± 25	5,176 ± 114	5,174 ± 124
LZU154	T0208⑤	AMS	Collagen from Bovidae	4,490 ± 25	5,165 ± 114	5,166 ± 123
Beta-539812	SNSZT0110H44	AMS	Collagen from Rhinoceros	4,450 ± 30	5,121 ± 147	5,089 ± 196
Beta-539813	SNSZT0309H113①*	AMS	Collagen from Bovidae	4,520 ± 30	5,181 ± 116	5,177 ± 127
Beta-539814	2013MCSIT0308④	AMS	Collagen from Bovidae	4,480 ± 30	5,162 ± 116	5,134 ± 155

*Sample included in aDNA analysis.

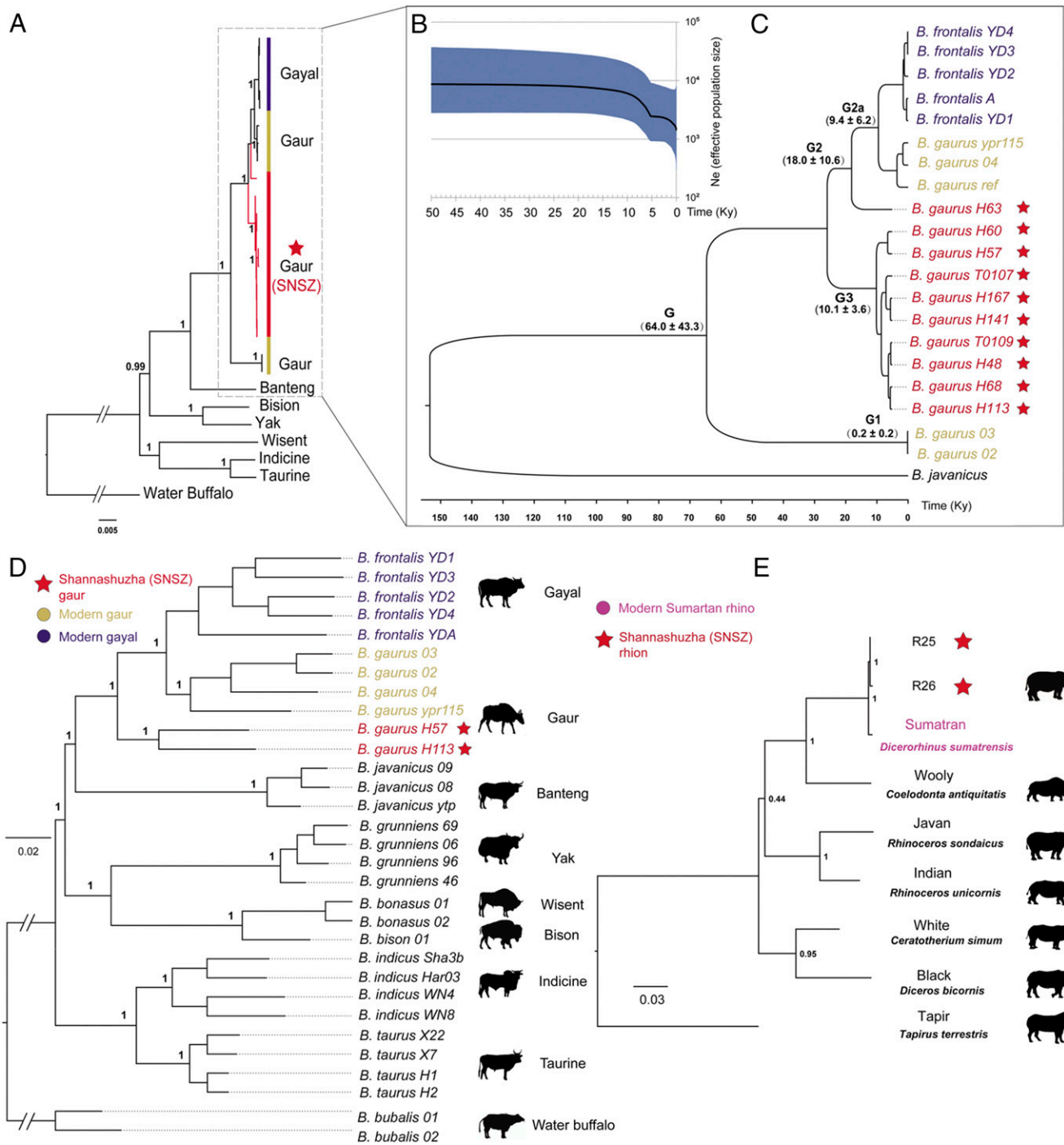


Fig. 2. Identification of ancient tropical animals (gaurs and rhinoceroses) in the margin of the Qinghai-Tibet Plateau. (A) Phylogeny of ancient and modern gaur mitogenomes. (B) Bayesian skyline plot showing the gaur and gayal effective population size trends. The y axis indicates the effective number of females, as inferred from our mitogenome dataset considering a generation time of 6 y. (C) An ML time scale of gaur and gayal mitogenomes. (D) The ML tree confirmed the phylogenetic affinities of present-day gaurs and ancient SNSZ gaurs using 8,961,232 autosomal sites. (E) Phylogeny of the rhinoceroses estimated from partial mitochondrial genome sequences, showing strong support for the grouping of ancient SNSZ rhinoceroses with Sumatran rhinoceroses.

affinity (*SI Appendix, Table S2*), which indicated a relatively small population size of the ancient bovid species. The genomic phylogenetic neighbor-joining (NJ) phylogeny (using 990,246 high-quality autosomal sites) clustered all 10 samples into a single clade with a clear divergence from the modern gaur and gayal populations (*SI Appendix, Fig. S5A*). We also constructed the genomic ML phylogenies of *Bos* species, including two of the relatively higher-coverage aDNA genomes (H113 and

H57) (using 8,961,232 high-quality autosomal sites and 72,720 coding region sites). Both the NJ and ML trees confirmed the above mtDNA results and were consistent with the topology of the *Bos* species (29) (Fig. 2D and *SI Appendix, Fig. S5*). We further examined the genetic relatedness between ancient SNSZ gaur and modern bovids by performing an outgroup *f*₃ analysis on whole-genome sequence data to measure the shared drift *f*₃(Buffalo; SNSZ, X). Our results corroborated the above ML

and NJ tree results and showed that the ancient samples are genetically most similar to modern Asian wild gaur (*SI Appendix, Table S6*).

For the two rhinoceros faunal remain samples, we performed shotgun sequencing and retrieved mtDNA data with a depth of 0.42× and 0.94×, covering 5,895 bp and 9,940 bp, respectively. To infer their species affiliation, we analyzed the two samples with the mitogenomes of six rhinoceros species (Sumatran [*D. sumatrensis*], white [*Ceratotherium simum*], black [*Diceros bicornis*], woolly [*Coelodonta antiquitatis*], Javan [*Rhinoceros sondaicus*], and Indian [*Rhinoceros unicornis*] rhinoceroses) and included one mitogenome of a Perissodactyla species (tapir, *Tapirus terrestris*) as an outgroup. The phylogenetic ML tree clearly proved that the two ancient samples were a sister clade of the Sumatran rhinoceros (Fig. 2E), which currently only inhabits the islands of Sumatra and Borneo in Indonesia.

Up to now, there has been no record that gaurs once inhabited relatively high latitudes in northern China, especially in the higher-altitude NETP. Our systematic aDNA dissection revealed that the present-day low-latitude tropical rainforest gaurs and Sumatran-like rhinoceroses once rambled over northern Asia as far north as the margin of the NETP at elevation up to ~2,300 m a.s.l. ~5,200 y B.P.

Reconstructing the SNSZ Gaur Population Dynamics and Testing Possible Gene Flow with the Other Bovid Species. To investigate the population dynamics of the SNSZ gaur population in the NETP, we constructed a Bayesian skyline plot (BSP) reflecting changes in the female effective population size through time using 21 mitogenomes including ancient gaur, modern gaur, and gyal mtDNAs plus one banteng (JN632605) as an outgroup. The BSP reconstruction showed a decreasing tendency in the effective female population size of gaurs and gayals beginning ~20,000 y B.P., coinciding with the LGM. A more rapid population decline of the gaur population size occurred ~5,000 y B.P., which persisted for a relatively long time afterward (Fig. 2B). The latter decline is congruent with the paleoclimatic record (Qinghai Lake) that the millennial-scale abrupt climate changes with the lowest summer temperature occurred in the NETP during 5,000 to 3,600 y B.P. (30) (Fig. 1), which might have resulted in the shrinking of many local wild animal populations (including the gaurs and Sumatran-like rhinoceros) and indicated distinct or massive escape from the habitat region and southward migration to lower-latitude warm regions.

We applied Patterson's *D*-statistic to further investigate the relatedness of the SNSZ gaur with extant bovid species and to test for past gene flow between the SNSZ gaur and other modern bovid species (31). The *D*-statistics demonstrates possible gene flow from SNSZ gaur into modern gaur (*SI Appendix, Table S7*). Furthermore, we did not detect gene flow between SNSZ gaur and yak, indicating possible niche isolation between ancient SNSZ gaur and yak ~5,200 y B.P. In contrast, we observed more complex introgression from modern gaur, gyal, and SNSZ gaur into Chinese indicine cattle and banteng introgression into Chinese indicine cattle (20) (*SI Appendix, Table S7*). Overall, our results are consistent with the absence of yak and domesticated cattle faunal remains at the SNSZ archaeological site (14), suggesting an isolated spatial-temporal ecological niche among gaur, yak, and domesticated cattle in the NETP during the late Neolithic period.

Discussion

The gaur, which also known as the "Indian bison," is the largest bovid species worldwide with an existing population size of ~20,000 and is designated as a vulnerable species on the International Union for Conservation of Nature (IUCN) Red List (25, 32). The global distribution of *B. gaurus* both historically and presently is restricted to the tropical and subtropical regions

throughout south and southeastern Asia, including in India, Nepal, Bhutan, Bangladesh, Myanmar, Thailand, China (Yunnan), Laos, Cambodia, Vietnam, and Malaysia (33) (Fig. 1). The northernmost gaur populations are found in the southern foothills of the Himalayas, with a latitude reaching northern latitudes of ~29° N in the hilly terrain of northeastern India (32, 33) (Fig. 1). In India, the *B. gaurus*-like faunal remains record includes an undated partial skull and horns, which were found in the order alluvium of the Narbada River in central India (34). *Bibos gaurus* remains, including skulls, horns, mandibles, and teeth found in south and southwest China, date to the Pleistocene (35). The Sumatran rhinoceros, which is also known as the hairy rhinoceros or Asian two-horned rhinoceros (*D. sumatrensis*), is the smallest rhinoceros of the Rhinocerotidae family member and is the only extant species of the genus *Dicerorhinus*. The Sumatran rhinoceros was once distributed throughout a continuous range of rainforests, swamps, and cloud forests in India, Bhutan, Bangladesh, Myanmar, Laos, Thailand, Malaysia, Indonesia, and southwest China; however, currently, there are only five substantial populations (four in Sumatra and one in Borneo), with fewer than 100 individuals left in the wild (36). Currently, yak and cattle are central to the economies of the Tibetan Plateau; therefore, most archaeological bovid remains in the NETP have been traditionally identified as Tibetan yak or cattle. In this study, we provide aDNA evidence for the presence of the gaur and Sumatran-like rhinoceroses in the margin region of the NETP during the late Neolithic (~5,200 y B.P.). These results suggest that the species geographic range likely extended up to an elevation of ~2,315 m a.s.l. and a northernmost latitude of ~34.49°N, updating our knowledge of the prehistoric geographic range of gaurs.

The Tibetan highlands host one of the world's largest pastoral ecosystems (37) and is home to a wide variety of animals that may have been exploited by early hunters (38). We compiled the archaeological and paleoclimatic data from the surroundings of the Tibetan Plateau and found that rhinoceroses and wild water buffalo appeared frequently throughout northern China during 8,000 to 6,000 y B.P., revealing a relatively warm and moist environment that could have sustained the survival of cold-sensitive Sumatran rhinoceroses. These zooarchaeological data are consistent with the paleoclimatic records of monsoonal China, in which the summer temperature and precipitation reached maximum values during the Holocene (39, 40) (Fig. 3 A, B, and E). Previous studies of SNSZ report the presence of badgers, snub-nosed monkeys, and Bambusoideae vegetation, all of which indicate a warmer and moister climate ~5,200 y B.P. (28). Gaur and Sumatran rhinoceroses currently inhabit tropical or subtropical low-latitude regions that have been significantly warmer than the SNSZ in the recent past (~6.5 °C and ~556 mm). Additionally, subtropical species, such as badger and wild water buffalo, were among zooarchaeological remains from the Guanzhong area in the central Loess Plateau, ~500 km to the east of the NETP, supporting higher temperature during the middle Yangshao period (~6,000 to 5,500 y B.P.) compared to the present temperature (41, 42). A comparison with high-resolution paleoclimate records from neighboring southwest China (Xingyun Lake) and the Loess Plateau (Gonghai Lake) further demonstrated that the summer temperature (mean July temperature) and annual precipitation were likely over ~2 °C and ~120 mm higher ~5,200 y B.P. than in the most recent past (Figs. 1 and 3 A and B). These climatic conditions could have facilitated the seasonal presence of gaur and Sumatran-like rhinoceroses in the SNSZ region. The optimum hydrothermal conditions during the Holocene occurred between ~7,500 and 5,500 y B.P., when hunting wildlife was the primary subsistence strategy in the NETP and adjacent regions (Fig. 3C). Additionally, rhinoceroses were also hunted in the western Loess Plateau during this period (Fig. 3E). This highlights the intimate connection

among climate change, the geographical distribution of wildlife, and human hunting behavior in northwest China during that period.

The intensification and expansion of rain-fed agriculture ~6,000 y B.P. altered the subsistence strategy in the Loess Plateau during the late Yangshao period, including the remarkable enhancement of significant animal husbandry that has dominated animal exploitation in this area since then (43). However, in the marginal areas of the mountainous environment, low human populations, combined with favorable water heating to ensure that the area became an ideal habitat for various wildlife including gaur and Sumatran-like rhinoceroses. The rich biodiversity in SNSZ and other regions of the NETP during the late sixth millennium facilitated the exploration of hunting, and therefore the emergence of a unique subsistence strategy dominated

by millet cultivation and game hunting. This lifestyle was evidently different from that in the middle-lower valleys of the Yellow River, which was based on millet cultivation and animal husbandry (44).

The diversity of wildlife in northern China declined during 5,000 to 4,000 y B.P. in comparison to the former millennium (Fig. 3C); however, hunting game continued to be an important strategy in the NETP above 2,500 m a.s.l. (9, 12) and probably contributed to the human influence on the local environment, such as the exploitation of woodlands during this period (45). The temperature and precipitation rapidly declined between 5,000 and 4,000 y B.P. (30, 39, 40). This climatic warm-humid/cold-dry transition was likely responsible for the rapid gaur population decline with an estimated onset of ~5,000 y B.P. (Fig. 2B) and for the change in human behavior with increased

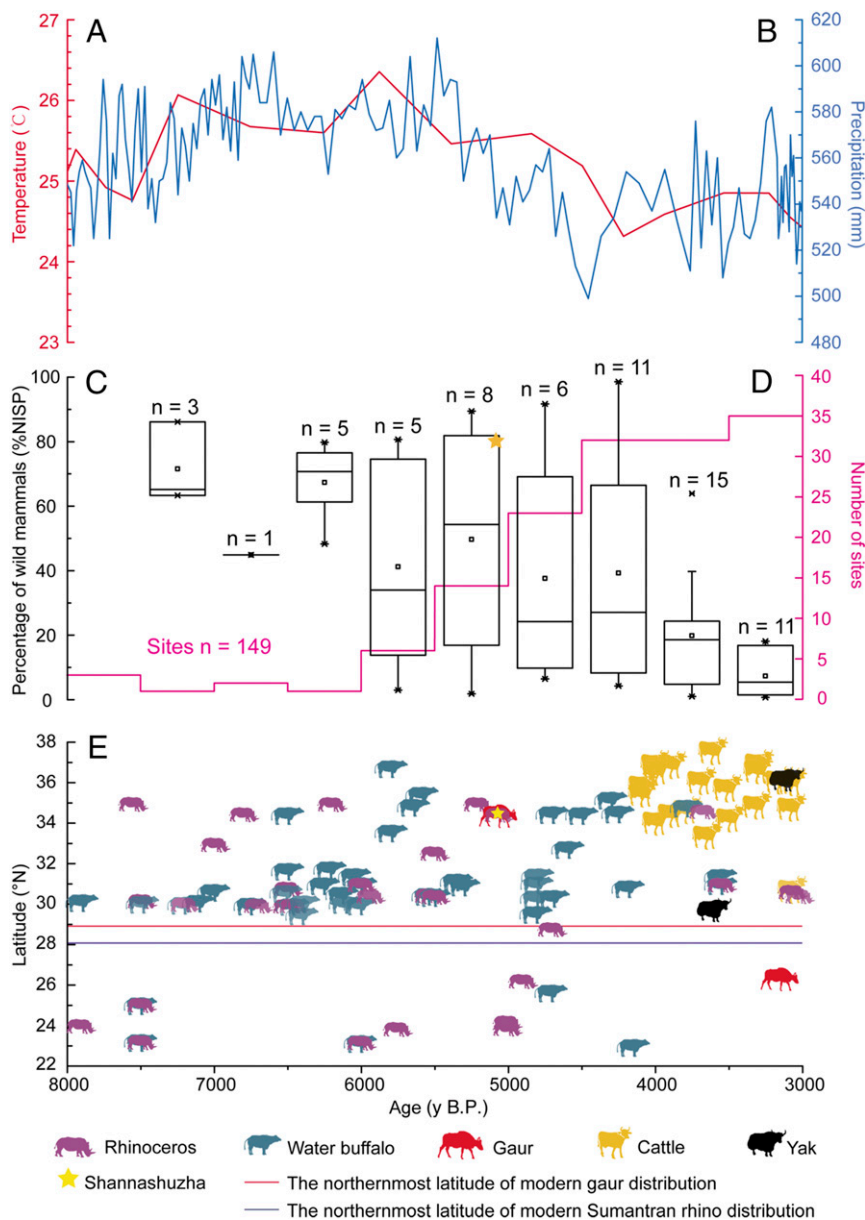


Fig. 3. The spatiotemporal distribution of unearthed remains of typical bovids and rhinoceroses compared with paleoclimate records, zooarchaeological data, and the number of dating sites. (A) Pollen-based mean July temperature reconstructed from Xingyun Lake (red line) (39). (B) Pollen-based annual precipitation reconstructed from Gonghai Lake (blue line) (40). (C) Variations of the percentage of NISP of wild mammals along the Yellow River basin, including the NETP, Loess Plateau, and North China Plain, during 8,000 to 3,000 y B.P. (D) Number of dated sites in the NETP and adjacent regions from 8,000 to 3,000 y B.P. (E) The historical distribution of typical bovids and rhinoceroses from 8,000 to 3,000 y B.P. through China (below 38° N) (67).

reliance on domesticated bovids. No remains of tropical wildlife including gaur and Sumatran-like rhinoceroses were identified from sites during this period in northern China, while gaur remains were reported from later southern sites (3,000 y B.P.) in the Yunnan province of southwestern China (46), suggesting that climate deterioration might have triggered the southward migration of cold-sensitive wild animals, which vacated niches for domesticated animals in the NETP (Fig. 3E).

We also demonstrate that the wild animal distribution along the Yellow River basin, including the NETP, Loess Plateau, and North China Plain, was associated with human activity (Fig. 3D). During 5,000 to 4,000 y B.P., although hunting game remained in northern China, the increasing human activity intensified the shrinking of wildlife populations, extinctions, and southward migrations and urged the transition of human subsistence strategies from hunter-gather to agricultural production. Based on the radiocarbon dates from archaeological sites in the NETP and the adjacent region, we found that the intensity of human colonization in that area showed an upward trend between 6,000 and 3,000 y B.P. (Fig. 3D). During 4,000 to 3,000 y B.P., the intensity of human settlements significantly increased (Fig. 3D). Livestock almost dominated animal exploitation in all regions of human settlements including the Tibetan Plateau, where there are vast pastures for domestic herbivorous animals, such as yaks, cattle, sheep/goats, and horses (9), which significantly reduced the habitats of wild animals. Thereafter, gaur and Sumatran-like rhinoceroses nearly vanished from areas north of ~34°N.

In conclusion, our genome-wide aDNA analysis reveals that the wild bovids in the late Neolithic in the NETP included *B. gaurus*, which has since been obscured by the distribution of modern yaks and cattle. Our findings push the historical gaur distribution from ~29°N to ~34°N. Additionally, by integrating aDNA with paleoclimatic and zooarchaeological evidence, our interdisciplinary investigation showed that the regional mid-Holocene warm climate period facilitated the low-latitude tropical animals undertaking northward expansion, enriching the biome diversity in the NETP, providing abundant hunting resources for local early human societies, and facilitating the exploration of hunting uniquely combined with millet cultivation. However, the subsequent climatic abruption and intensified human activities during 5,000~4,000 y B.P. narrowed the spaces for wildlife. Gradually, hunting game was replaced by herding activities after 4,000 y B.P. Indeed, after 3,600 y B.P. humans extensively and permanently settled on the high-altitude areas with cold-tolerant agropastoral economies (9). Both climatic change and human activities contributed to the disappearance of gaur and Sumatran-like rhinoceros from the middle and high latitudes, eventually shaping their modern tropical biogeographic distributions. Additionally, our aDNA analysis supports the rapid turnover of different bovid species in the NETP during the mid-Holocene. Further aDNA studies, combined with multidisciplinary approaches from more archaeological sites in northern Asia are necessary to further our understanding of the past interactions among climate change, biogeography, and human activity.

Materials and Methods

Bovidae Bone Remains Sampling from the SNSZ Archaeological Site. The archaeological site of SNSZ dates to ~5,280 to 5,050 cal y B.P. and is located at an altitude of 2,323 m a.s.l. in the margin region between the NETP and the Loess Plateau of northwestern China. The composition of faunal remains at this archaeological site is diverse (SI Appendix, Table S1). Species identified via morphology include rabbits (*Lepus capensis*), bamboo rats (*R. pruinosus*), Siberian roe deer (*Capreolus pygargus*), barking deer (*Muntiacus aurus*), red deer (*Cervus elaphus*), sika deer (*Cervus nippon*), Bovidae, badgers (*Meles meles*), pigs (*Sus scrofa domestica*), Chinese goral (*Naemorhedus goral*), and Rhinocerotidae (14). The specific species identification of Bovidae and Rhinocerotidae specimens via morphological approaches has not been possible.

Here, we randomly selected 10 Bovidae and 2 Rhinocerotidae samples (SI Appendix, Table S2 and Fig. S1) to perform molecular identification.

Radiocarbon Dating. We collected five different animal bone fragments in total for the AMS radiocarbon dating, and one Bovidae sample of them was also used for aDNA extraction and species identification (Table 1). Two animal collagen samples from one deer and one gaur were extracted and pretreated at the Chronology Laboratory of the Ministry of Education Key Laboratory of Western China's Environmental Systems, Lanzhou University. Then, these samples were sent to Peking University in Beijing for the dating measurement. The other three samples from two gaurs and one rhinoceros were dated at Beta Analytic, Miami, CA. All chronological data were calibrated by the Calib radiocarbon calibration program (v.7.0.2) (47) and the IntCal13 calibration curve. All reported ages are relative to AD 1950 (referred to as "cal y B.P.")

aDNA Extraction, Library Preparation, Genome Capture, and Sequencing. We collected 12 bone samples to perform molecular identification of these faunal remains from the SNSZ site (SI Appendix, Fig. S1 and Table S2). aDNA extraction, the quantification of DNA preservation, and double-stranded DNA library (DSL) construction were performed following previous reports (48, 49) in the aDNA dedicated laboratory of the CGG at Kunming Institute of Zoology, Chinese Academy of Sciences. In brief, prior to DNA extraction we conducted ultraviolet (UV) irradiation on the samples for ~2 h and removed a surface layer using a sterile dentistry drill. For each sample, we drilled ~200 mg of bone powder for aDNA extraction. aDNA extraction was performed using the silica adsorption protocol as in previous reports (48, 49), which resulted in 200 μ L of extraction for each sample.

For the screening of DNA preservation we used 10 μ L of extract per sample to build DSLs, using a commercial kit from New England Biolabs (50). We performed the PCRs with a final volume of 50 μ L using KAPA uracil+ polymerase (Kapa Biosystems), which can incorporate nucleotides across uracils and preserves the deamination-induced damage patterns that are an indication of authentic aDNA (51). We sequenced the constructed DSL aDNA libraries (including all later captured genomic libraries) using the Illumina HiSeq X Ten (PE-150) platform (WuXi NextCode Genomics Co., Ltd.). For the 10 Bovidae samples, we treated the remaining extract with uracil-DNA-glycosylase to remove uracil residues from the DNA to leave abasic sites and applied enzyme endonuclease VIII (Endo VIII), which cuts the DNA at the 5' and 3' sides of abasic sites. Following the treatment, DSLs were then built as described above. We then performed genomic capturing to these libraries using RNA baits transcribed from cattle genomic DNA as in previously reported methods (52, 53). The PCRs of both precapture and postcapture samples was conducted using the KAPA HiFi Hot Start Polymerase protocol (Kapa Biosystems).

Process of Ancient Data Mapping, Alignment, Filtering, and mtDNA Assembly. Adapter sequences of the paired-end reads were identified and removed using AdapterRemoval version 2.2.0 (54). Reads were separately aligned to mitogenome references of the taurine cattle (V00654.1) and gaur (NC_024818.1) using Burrows–Wheeler Alignment (BWA) (55). To improve the alignment to the circular mtDNA genome, a 30-bp sequence from the end was attached to the beginning. Reads were subsequently filtered for PCR duplicates and a mapping quality <30 using SAMtools (v. 0.1.19) (56). Four resequenced modern gaurs and five resequenced modern gayals were aligned to the same *B. gaurus* mitogenome reference (SI Appendix, Table S5). For the two rhino samples, we mapped the reads to the *R. unicornis* mitogenome reference (NC_012684.1). mtDNA coverages were calculated by Qualimap (v. 2.2) (SI Appendix, Table S3).

We retrieved the mtDNA data of ancient gaur with the sequence depths range from 9.05 \times to 1,703.55 \times (SI Appendix, Table S3) and the coverage range from 5,895-bp to 9,940-bp mtDNA for the two Rhinocerotidae samples. The average length of the Bovidae and Rhinocerotidae molecules were 51 to 80 bp and 75 to 77 bp, respectively, the TDR of all of the shotgun sequenced samples were >10%, and the maximum mapping rate was 3.75% (T0109), all of which indicated typical aDNA characteristics (SI Appendix, Table S2). The final mtDNA BAM files were used with Mapping Iterative Assembler v. 1.0 to assemble mtDNA consensus sequences and manually and visually inspected for all mutations against the sequence.

Alignment of Ancient Bovid NGS Genomic Reads to the *B. taurus* Genome. All raw reads were processed through a standardized pipeline adapted for the ancient samples. The adapter sequences of the paired-end reads were identified and removed using AdapterRemoval version 2.2.0 (54). We merged read pairs for which the expected index was observed, required an

overlap of at least 11 bp. Because there is no *B. gaurus* reference genome, the bovine reference genome (ARS-UCD1.2) with the addition of the Y chromosome from BosTau7 was used as a reference. Alignments were performed using the Burrows–Wheeler Alignment Tool (55) (v. BWA 0.7.5a-r405) with the parameter `aln -l 16500 -n 0.01`, and the parameter `samse` with the option `-r` to define the read groups and to produce unfiltered SAM files, which were subsequently converted to BAM files using the command `samtools view -Sb`. The BAM files were sorted using `SAMtools` (v. 0.1.19) (56). The BAM files were merged using `picard-tools` (v. 1.129), and indel realignment was performed using the Genome Analysis Tool Kit (GATK; v. 3.8) (57). Duplicates were removed using `Picard-tools` (v. 1.128, broadinstitute.github.io/picard/) (MarkDuplicates REMOVE_DUPLICATES = true) prior to indel realignment. The samples were filtered using `SAMtools` to remove unaligned reads (view -F4) and for mapping the quality of Q25 (view -q25). Quality control parameters of the alignment sequencing data and coverage statistics were calculated using `Qualimap` (v. 2.2) (58).

Alignment of Modern Bovine NGS Genomic Reads to the *B. taurus* Genome. We generated four whole genomes of *B. frontalis* and combined these data with previously published genomes from modern bovines for phylogenetic analysis and species identification (SI Appendix, Table S5), including four *B. taurus*, four *B. indicus*, three *B. javanicus*, five *B. frontalis*, four *B. gaurus*, four *B. grunniens*, one *B. bison*, two *B. bonasus*, and two *B. bubalis*. For the modern gaur and gayal data, all animals were assigned to five geographical groups following their sources: American zoo gaur, European zoo gaur, Asian wild gaur, Southeast Asian wild gayal, and Chinese gayal (SI Appendix, Table S5). These data were used for “high confidence” variant datasets.

We further combined other 31 indicine cattle from South China and South Asia to investigate the potential pattern and consequences of gene flow between ancient species and modern species (SI Appendix, Table S5). All passed quality-filtered reads were aligned to the *B. taurus* reference genome ARS-UCD1.2 with the addition of the Y chromosome from BosTau7 using `bwa mem`. Duplicated reads were filtered using `Picard-tools` (v. 1.128). Reads around indels were realigned by `GATK` (v 3.8) (57).

Variant Discovery and Genotyping. `Bcftools` `mpileup` and `call` were used to call variants from the “high confidence” sample set (`-q 30 -C 50 -Q 20 -B -a FORMAT/AD, FORMAT/SP, FORMAT/ADF, FORMAT/ADR`) and generate `vcf` files (`-O z -m -o`). Indels and any variants within 3 bp near indels were removed using the `bcftools` filter. Repeat regions as defined by the UCSC Browser and Repeat-Masker files were removed (59) (genome.ucsc.edu). Tri- and quad-allelic sites were removed. Variants with coverages of twice the mean coverage that were marked as missing (“./.”). Heterozygous variants present in a single individual or more than 75% of individuals were removed. Variant positions with missing data in any individual were then removed, resulting in a dataset of 45,964,584 sites.

For samples H113 and H57 with $>2\times$ mean coverage, the above defined “high confidence” sites were called. The sites were called using `bcftools mpileup` with the same options but without recalibration (`bcftools mpileup -B`) and without filtering for variant sites with `bcftools`. After indels and sites within 3 bp of the indels were removed, tri- and quad-allelic sites were removed. Sites were set to missing as defined above (greater than twice the mean coverage). Individuals were then pseudodiploidized by randomly sampling a read at each site and setting that individual as homozygous for that allele. Variant positions with missing data in any individual were then removed. All transitions were removed. This call set was then merged with the Moderns set to create an “Ancients and Moderns” dataset, resulting in a dataset of 8,961,232 sites. This dataset was used for species identification.

For samples with less than $2\times$ depth, no minimum coverage filter was imposed and a maximum of 4 read coverage per site was permitted. Individuals were then pseudodiploidized by randomly sampling a read at each site and setting that individual as homozygous for that allele. Variant positions with 50% missing data in 10 ancient samples were then removed. All transitions were removed. This call set was then merged with the “Ancients and Modern” set to create a “Low Coverage Ancients and Modern” dataset, resulting in 990,246 sites. This dataset was used for species identification for all SNSZ samples.

We combined “Ancients and Moderns” and 31 other previously published indicine cattle genomes to investigate the gene flow between ancient genomes and modern genomes. We used the above criteria to genotype and filter single-nucleotide polymorphisms (SNPs), resulting in 4,893,675 sites.

Phylogeny Construction and Demographic Inferences with Gaur Mitogenome Sequences. Gaur mitogenome sequences were aligned using `ClustalW v2` (60). The control region, as well as any positions in the alignment that contained

missing data, were removed. The resulting alignment was manually annotated using gaur (GenBank: NC_024818.1) as the reference. The consensus mitochondrial genomes of the 10 ancient gaur sequences, four *B. gaurus* and five *B. frontalis* genomes (newly assembled) were aligned with the available mitogenomes of six Bovine species, including the mitogenomes of one *B. taurus*, one *B. indicus*, one *B. javanicus*, one *B. grunniens*, one *B. bison*, one *B. bonasus*, and one *B. bubalis* (SI Appendix, Table S4).

BEAST analysis was performed with BEAST (2.6.1) (61). To calibrate the molecular clock, we built a tree by including ancient gaur, modern gaur, and gayal mtDNAs plus one banteng (JN632605) as an outgroup. The coalescence ages of the ancient gaurs (5.2 ± 0.15 ky; 95% CI: 4.94 to 5.46 ky) were used as an internal (recent) calibration point. The major haplogroups were considered as monophyletic to calculate their age estimates. We then obtained a BSP from the gaur phylogeny by running 50 million iterations with samples drawn every 1,000 steps.

Rhinoceros mitogenome sequences were aligned using `ClustalW v2` (60). The resulting alignment (3,452 bp in length) was manually annotated in `Geneious` using the modern Sumatran rhinoceros (GenBank: NC_012684.1) as a reference. For interspecies comparison between ancient SNSZ and modern rhinoceros, mitogenomes for Indian, Javan, Sumatran, woolly, and white rhinoceros were downloaded and aligned with the two SNSZ specimens using `ClustalW v2`. Alignment columns containing missing data were not considered to enable direct comparison of genetic distances within extant species with those estimated from SNSZ assemblies. The alignment contained five rhinoceros subspecies, including one *R. unicornis*, one *R. sondaicus*, one *C. simum*, one *C. antiquitatis*, and one *D. sumatrensis* (SI Appendix, Table S4). The GTR+G model of nucleotide substitution was selected by comparing the Bayesian information criterion scores in `ModelGenerator v0.85` (62). An ML tree of 3,452 bp length alignment was computed using `MEGA7.0` with 1,000 bootstrapping replicates (SI Appendix, Fig. S5) (63).

Phylogenetic Inference Using a Supermatrix of Nuclear Coding Sequences. An NJ phylogenetic tree of 10 SNSZ samples and other species from the *Bos* genus was also constructed using the “Low Coverage Ancients and Modern” dataset with 990,246 sites.

The phylogenetic relationships of two ancient samples (H113 and H57) and nine modern species were inferred by the ML method with 100 bootstraps and the NJ method using the “Ancients and Modern” dataset. The low-coverage genomes of other SNSZ gaurs were not included in this analysis. We used all 8,961,232 sites and variants within coding sequences (CDs) separately (SI Appendix, Fig. S5). The protein-coding gene annotation information was performed according to the annotation of the current cattle reference ARS-UCD1.2. We obtained 72,720 sites within the CDs. ML phylogenetic inference was performed using `RaxML v8.1.3` (64) using default parameters. The resulting tree was rooted using water buffalo (*B. bubalis*).

A total of 8,961,232 autosomal SNPs was selected to construct an NJ tree including the two high-coverage samples with `PLINK` using the matrix of pairwise genetic distances (SI Appendix, Fig. S5).

We further examined the genetic relatedness between SNSZ species and modern gaur and gayal by performing the outgroup f_3 statistic to measure the shared drift using the `ADMIXTOOLS` (version 6.0) package and `qp3Pop` program. The test (Buffalo; SNSZ gaur; X) was performed utilizing the “Ancients and Modern” dataset, rotating X through 5 modern gaur and gayal populations.

Sex Determination and Individual Genetic Relatedness for Bovine Faunal Remains from the SNSZ Site. The ratio of mapped reads to autosomes and X and Y chromosomes could be used to infer sex (65). We used this method to infer the sexes of the 10 samples with 990,246 sites, and we found that the sets included five male and five female samples, respectively (SI Appendix, Table S2). For the three relatively higher genomic coverage samples H113, H57, and H48, we analyzed the kinship using `KING` (66) to assess their relatedness, and we found that they possessed fourth- to third-generation affinity (SI Appendix, Table S2), which indicated a relatively small population size of the ancient bovine species.

Introgression Events Test among SNSZ Gaur with Other Bovine Species. `ADMIXTOOLS` (version 6.0) software was used to determine relationship between the ancient SNSZ gaur and modern bovine groups using 4,893,675 autosomal sites without transitions. We used Patterson’s *D*-statistic to test whether ancient SNSZ gaur shared more derived alleles with modern bovines using the `qp-Dstat` program (SI Appendix, Table S7).

Compilation of the Archaeologically Excavated Large Animals, Paleoclimate, and Human Activity Records from Northern China. We created a database of the rhino, gaur, water buffalo, yak, and cattle presence through northern China (below 38° N). The whole database and references to the original studies are available in [SI Appendix, Table S8](#). The pollen-based mean July temperature reconstructed from Xingyun Lake and annual precipitation reconstructed from Gonghai Lake were also collected. The NISP of wild mammals and radiocarbon dates along the Yellow River basin from 8,000 to 3,000 y B.P. were collected (67) ([SI Appendix, Table S9](#)).

Data Availability. All of the final bam files reported in this study have been deposited in the Genome Sequence Archive in the National Genomics Data Center, Beijing Institute of Genomics (China National Center

for Bioinformatics), Chinese Academy of Sciences, under accession number [CRA002649](#) and are publicly accessible at <https://bigd.big.ac.cn/gsa/gsa/>.

ACKNOWLEDGMENTS. This study was supported by the National Natural Science Foundation of China (NSFC) 31601018 and 31871258 to X.Z., 41825001 to G.D., Yunnan provincial “ten thousand people plan” “youth top talent” project (2019) to X.Z., 41620104007 (NSFC) to F.C., G.D., and X.Z., and 41901089 (NSFC) to L.R. This study was also supported by the Open Project (GREKF20-12) of State Key Laboratory of Genetic Resources and Evolution, Chinese Academy of Sciences to N.C. This study also received support from the Fondazione Cariplo (project 2018-2045 to A.A.) and the Italian Ministry of Education, University and Research Dipartimenti di Eccellenza Program 2018–2022 and PRIN 20174BTC4R (to A.A.).

1. J. R. Stewart, C. B. Stringer, Human evolution out of Africa: The role of refugia and climate change. *Science* **335**, 1317–1321 (2012).
2. A. Timmermann, T. Friedrich, Late Pleistocene climate drivers of early human migration. *Nature* **538**, 92–95 (2016).
3. A. Cooper *et al.*, PALEOECOLOGY. Abrupt warming events drove Late Pleistocene Holarctic megafaunal turnover. *Science* **349**, 602–606 (2015).
4. A. M. Rosen, I. Rivera-Collazo, Climate change, adaptive cycles, and the persistence of foraging economies during the late Pleistocene/Holocene transition in the Levant. *Proc. Natl. Acad. Sci. U.S.A.* **109**, 3640–3645 (2012).
5. J. Diamond, P. Bellwood, Farmers and their languages: The first expansions. *Science* **300**, 597–603 (2003).
6. N. L. Boivin *et al.*, Ecological consequences of human niche construction: Examining long-term anthropogenic shaping of global species distributions. *Proc. Natl. Acad. Sci. U.S.A.* **113**, 6388–6396 (2016).
7. Z. Zhao, New archaeobotanic data for the study of the origins of agriculture in China. *Curr. Anthropol.* **52** (suppl. 4), S295–S306 (2011).
8. L. Barton *et al.*, Agricultural origins and the isotopic identity of domestication in northern China. *Proc. Natl. Acad. Sci. U.S.A.* **106**, 5523–5528 (2009).
9. F. Chen *et al.*, Agriculture facilitated permanent human occupation of the Tibetan Plateau after 3600 B.P. *Science* **347**, 248–250 (2015).
10. G. Dong *et al.*, Spatial and temporal variety of prehistoric human settlement and its influencing factors in the upper Yellow River valley, Qinghai Province, China. *J. Archaeol. Sci.* **40**, 2538–2546 (2013).
11. Y. Li *et al.*, Neolithic millet farmers contributed to the permanent settlement of the Tibetan Plateau by adopting barley agriculture. *Natl. Sci. Rev.* **6**, 1005–1013 (2019).
12. L. Ren *et al.*, Dating human settlement in the east-central Tibetan Plateau during the Late Holocene. *Radiocarbon* **60**, 137–150 (2017).
13. L. Ren, “A study on animal exploitation strategies for the late Neolithic to Bronze Age in northeastern Tibetan Plateau and its surrounding areas [in Chinese],” PhD thesis, Lanzhou University, Lanzhou, China (2017).
14. W. Dong, C. An, W. Fan, H. Li, X. Zhao, Stable isotopic detection of manual intervention among the faunal assemblage from a Majiayao site in NW China. *Radiocarbon* **58**, 311–321 (2016).
15. Y. Hu, “Research of charred botanical remains from Shannashuzha Site in Gansu Province [in Chinese],” Master’s thesis, Northwest University, Xi’an, China (2015).
16. G. Dong, L. Wang, Y. Cui, R. Elston, F. Chen, The spatiotemporal pattern of the Majiayao cultural evolution and its relation to climate change and variety of subsistence strategy during late Neolithic period in Gansu and Qinghai Provinces, northwest China. *Quat. Int.* **316**, 155–161 (2013).
17. D. Y. Yang, L. Liu, X. Chen, C. Speller, Wild or domesticated: DNA analysis of ancient water buffalo remains from north China. *J. Archaeol. Sci.* **35**, 2778–2785 (2008).
18. D. Cai *et al.*, New ancient DNA data on the origins and spread of sheep and cattle in northern China around 4000 BP. *Asian Archaeology* **2**, 51–57 (2018).
19. D. Cai *et al.*, Ancient DNA reveals evidence of abundant aurochs (*Bos primigenius*) in Neolithic Northeast China. *J. Archaeol. Sci.* **98**, 72–80 (2018).
20. N. Chen *et al.*, Whole-genome resequencing reveals world-wide ancestry and adaptive introgression events of domesticated cattle in East Asia. *Nat. Commun.* **9**, 2337 (2018).
21. G. Dong *et al.*, Chronology and subsistence strategy of nuomuhong culture in the Tibetan Plateau. *Quat. Int.* **426**, 42–49 (2016).
22. J. Marsicek, B. N. Shuman, P. J. Bartlein, S. L. Shafer, S. Brewer, Reconciling divergent trends and millennial variations in Holocene temperatures. *Nature* **554**, 92–96 (2018).
23. C. C. Routson *et al.*, Mid-latitude net precipitation decreased with Arctic warming during the Holocene. *Nature* **568**, 83–87 (2019).
24. S. A. Marcott, J. D. Shakun, P. U. Clark, A. C. Mix, A reconstruction of regional and global temperature for the past 11,300 years. *Science* **339**, 1198–1201 (2013).
25. J. Duckworth, K. Sankar, A. Williams, N. Samba Kumar, R. Timmins, *Bos gaurus*. *The IUCN Red List of Threatened Species* 2016: e.T2891A46363646 (IUCN, 2016).
26. N. J. Van Strien *et al.*, *Dicerorhinus sumatrensis*. *The IUCN Red List of Threatened Species* 2008: e.T6553A12787457 (IUCN, 2008).
27. T. J. Foote *et al.*, *Asian Rhinos: Status Survey and Conservation Action Plan*, (IUCN, Cambridge, UK, 1997).
28. H. Li *et al.*, Woodland vegetation composition and prehistoric human fuel collection strategy at the Shannashuzha site, Gansu Province, northwest China, during the middle Holocene. *Veg. Hist. Archaeobot.* **26**, 213–221 (2017).
29. D. Wu *et al.*, Pervasive introgression facilitated domestication and adaptation in the *Bos* species complex. *Nat. Ecol. Evol.* **2**, 1139–1145 (2018).
30. J. Hou *et al.*, Large Holocene summer temperature oscillations and impact on the peopling of the northeastern Tibetan Plateau. *Geophys. Res. Lett.* **43**, 1323–1330 (2016).
31. N. Patterson *et al.*, Ancient admixture in human history. *Genetics* **192**, 1065–1093 (2012).
32. F. S. Ahrestani, *Bos frontalis* and *Bos gaurus* (Artiodactyla: Bovidae). *Mamm. Species* **50**, 34–50 (2018).
33. A. Choudhury, Distribution and conservation of the Gaur *Bos gaurus* in the Indian subcontinent. *Mammal Rev.* **32**, 199–226 (2002).
34. SpiiSBury, On *Bos gaurus*. *J. Asiat. Soc. Bengal* **9**, 551 (1840).
35. E. H. Colbert, Pleistocene mammals from the limestone fissures of Szechwan, China. *Bull. Am. Mus. Nat. Hist.* **102**, 1–134 (1953).
36. W. Pusparini, P. R. Sievert, T. K. Fuller, T. O. Randhir, N. Andayani, Rhinos in the parks: An island-wide survey of the last wild population of the sumatran rhinoceros. *PLoS One* **10**, e0136643 (2015).
37. G. Miehle *et al.*, How old is pastoralism in Tibet? An ecological approach to the making of a Tibetan landscape. *Palaeogeogr. Palaeoclimatol. Palaeoecol.* **276**, 130–147 (2009).
38. G. B. Schaller, *Wildlife of the Tibetan Steppe*, (University of Chicago Press, 2000).
39. D. Wu *et al.*, Decoupled early Holocene summer temperature and monsoon precipitation in southwest China. *Quat. Sci. Rev.* **193**, 54–67 (2018).
40. F. Chen *et al.*, East Asian summer monsoon precipitation variability since the last deglaciation. *Sci. Rep.* **5**, 11186 (2015).
41. S. Hu, W. Wang, X. Guo, W. Zhang, M. Yang, The analysis of the faunal remains from the moat’s west gate at the Yangguanzhai site, Gaoling County, Shaanxi Province [in Chinese]. *Archaeol. Cultural Relics* **6**, 97–107 (2011).
42. S. Hu, Q. Yang, M. Yang, The analysis of animal remains from the Xinglefang site in Huayin County, Shaanxi Province [in Chinese]. *Archaeol. Cultural Relics* **6**, 117–125 (2011).
43. Y. Qu, K. Hu, M. Yang, J. Cui, Biological evidence for human subsistence strategy in the Guanzhong area during the Neolithic Period [in Chinese]. *Acta Polym. Sin.* **37**, 96–109 (2018).
44. F. Wang *et al.*, Reconstructing the food structure of ancient coastal inhabitants from Beiqian village: Stable isotopic analysis of fossil human bone. *Chin. Sci. Bull.* **57**, 2148–2154 (2012).
45. F. Liu, “Human wood utilization strategy in the Northeast of Tibetan Plateau during the Neolithic and Bronze Age [in Chinese],” PhD thesis, Lanzhou University, Lanzhou, China (2019).
46. J. Wang, “A zooarchaeological study of the Haimenkou Site, Yunnan Province, China,” PhD thesis, La Trobe University, Bundoora, VIC, Australia (2012).
47. M. Stuiver, P. J. Reimer, Extended 14C data base and revised calib 3.0 14C age calibration program. *Radiocarbon* **35**, 215–230 (1993).
48. N. Rohland, M. Hofreiter, Ancient DNA extraction from bones and teeth. *Nat. Protoc.* **2**, 1756–1762 (2007).
49. J. Dabney, M. Meyer, Extraction of highly degraded DNA from ancient bones and teeth. *Methods Mol. Biol.* **1963**, 25–29 (2019).
50. M. Meyer, M. Kircher, Illumina sequencing library preparation for highly multiplexed target capture and sequencing. *Cold Spring Harb. Protoc.* **2010**, pdb prot5448 (2010).
51. B. Mühlemann *et al.*, Ancient hepatitis B viruses from the bronze age to the medieval period. *Nature* **557**, 418–423 (2018).
52. J. M. Enk *et al.*, Ancient whole genome enrichment using baits built from modern DNA. *Mol. Biol. Evol.* **31**, 1292–1294 (2014).
53. M. L. Carpenter *et al.*, Pulling out the 1%: Whole-genome capture for the targeted enrichment of ancient DNA sequencing libraries. *Am. J. Hum. Genet.* **93**, 852–864 (2013).
54. M. Schubert, S. Lindgreen, L. Orlando, AdapterRemoval v2: Rapid adapter trimming, identification, and read merging. *BMC Res. Notes* **9**, 88 (2016).
55. H. Li, R. Durbin, Fast and accurate short read alignment with Burrows-Wheeler transform. *Bioinformatics* **25**, 1754–1760 (2009).

56. H. Li *et al.*; 1000 Genome Project Data Processing Subgroup, The sequence alignment/ map format and SAMtools. *Bioinformatics* **25**, 2078–2079 (2009).
57. A. McKenna *et al.*, The genome analysis toolkit: A mapReduce framework for analyzing next-generation DNA sequencing data. *Genome Res.* **20**, 1297–1303 (2010).
58. F. García-Alcalde *et al.*, Qualimap: Evaluating next-generation sequencing alignment data. *Bioinformatics* **28**, 2678–2679 (2012).
59. D. Karolchik *et al.*, The UCSC table browser data retrieval tool. *Nucleic Acids Res.* **32**, D493–D496 (2004).
60. M. A. Larkin *et al.*, Clustal W and clustal X version 2.0. *Bioinformatics* **23**, 2947–2948 (2007).
61. R. Bouckaert *et al.*, BEAST 2: A software platform for Bayesian evolutionary analysis. *PLoS Comput. Biol.* **10**, e1003537 (2014).
62. T. M. Keane, C. J. Creevey, M. M. Pentony, T. J. Naughton, J. O. McInerney, Assessment of methods for amino acid matrix selection and their use on empirical data shows that ad hoc assumptions for choice of matrix are not justified. *BMC Evol. Biol.* **6**, 29 (2006).
63. S. Kumar, G. Stecher, K. Tamura, MEGA7: Molecular evolutionary genetics analysis version 7.0 for bigger datasets. *Mol. Biol. Evol.* **33**, 1870–1874 (2016).
64. A. Stamatakis, RAxML version 8: A tool for phylogenetic analysis and post-analysis of large phylogenies. *Bioinformatics* **30**, 1312–1313 (2014).
65. P. Skoglund, J. Stora, A. Götherström, M. Jakobsson, Accurate sex identification of ancient human remains using DNA shotgun sequencing. *J. Archaeol. Sci.* **40**, 4477–4482 (2013).
66. A. Manichaikul *et al.*, Robust relationship inference in genome-wide association studies. *Bioinformatics* **26**, 2867–2873 (2010).
67. G. Dong, R. Li, M. Lu, D. Zhang, N. James, Evolution of human–environment interactions in China from the late paleolithic to the bronze age. *Prog. Phys. Geogr.* **44**, 233–250 (2020).